Influence of in situ photo-induced silver nanoparticles on the ageing of acrylate materials

H.B. B Zouari, M. Dabert, L. Asia, P. Wong-Wah-Chung, M. Baba, L. Balan, Y. Israëli

Influence of *in situ* photo-induced silver nanoparticles on the ageing of acrylate materials

H. B. Zouari[a], M. Dabert[b], L. Asia[c], P. Wong-Wah-Chung[c], M. Baba[a], L. Balan[b,*], Y. Israëli[a,*]

[a]*Université Clermont-Auvergne-CNRS-SIGMA, Institut de Chimie de Clermont-Ferrand, Campus des Cézeaux, 24 Avenue Blaise Pascal, TSA 60026, CS 60026, 63178 Aubière Cedex, France*

[b]*Conditions Extrêmes et Matériaux : Haute Température et Irradiation - UPR3079 CNRS, Université Orléans, 45071 Orléans, France*

[c]*Aix-Marseille Université, LCE, CNRS, Marseille, France*

*Email: *yael.israeli@uca.fr, *lavinia.balan@cnrs-orleans.fr*

ABSTRACT

The present work aims to investigate the impact of a low amount of photo-induced silver nanoparticles (0.2 and 0.4 wt.% of Ag NPs) on the stability of acrylate materials (carriers of ester and ether groups) under the combined effect of oxygen and light. Different techniques were implemented to monitor the structural changes at different scales. The determination of the influence of AgNPs required a preliminary investigation of the pure acrylate polymer under the same experimental conditions. The polymer underwent a post-polymerization of the residual vinyl groups and a photo-oxidative degradation. This degradation induced chemical modifications evidenced by infrared spectroscopy and architectural changes resulting from chain scission reactions. These reactions were not only responsible for the steaming of volatile organic compounds, detected by HS-SPME/GC-MS but also for the increase in mesh size controlled by thermoporosimetry.

As regards the polymer/Ag NPs composite, the higher the amount of filler dispersed in the matrix, the greater the rate of degradation. This behaviour was due to the photocatalytic effect of Ag NPs, regardless of the loading in nanoparticles. As a result of irradiation, the nanoparticles migrate to the surface of the film and coalesce, thus inducing an increase in size distribution and a gradient structuring as revealed by TEM analysis.

The outcomes of this investigation are important for the development of new composite material with new functionalities (antibacterial, optical, conductive properties) for industrial applications as in textile industry.

Keywords : silver nanoparticle, nanoparticle migration, acrylate photopolymer, photo-oxidation, composite material

1. Introduction

Innovative applications of composite materials, e.g. in aerospace, automobile, marine industry, sporting equipment [1,2], biosensors [3,4] or for biomedical purposes [5], permanently stimulate the development of new sustainable materials capable of providing new functionalities. Among many types of nanoparticles (NPs) available and dispersible in a polymer matrix, silver nanoparticles (AgNPs) were tested and evaluated. These nanoparticles are capable of imparting antimicrobial activity [6,7], or optical [8] and conductive [9,10] properties to the polymer material. However, the key characteristic of this type of material remains the durability of the polymeric matrix in the specific environment in which it is to be used. Indeed, it is well known that, in general, the combination of oxygen, humidity and sunlight leads to degradation and consequently to chemical and architectural modifications of the macromolecular chains (chain scission and crosslinking) which strongly affect the use properties of the composite polymer material.

However, there was great interest in the remediation of polluting industrial waste. The use of silver nanoparticles was a promising solution to overcome this problem as they exhibited photocatalytic potential to degrade water effluents under sunlight [11-16].This photocatalytic effect could be a disadvantage to a long term stability of a composite material. The following examples of earlier studies of polymer/Ag NPs composites illustrate the influence of the

nanofillers on the photochemical and thermochemical stability of various polymers. In the case of high-density polyethylene (HDPE), Ag NPs acted as a stabilizer when the composite material was exposed to UV irradiation at 280 nm [17]. The higher the NPs loading (0.5 to 5 wt %), the lower was the concentration of products resulting from the oxidative chain scission due to oxidation. When the amount of NPs was at its highest, the high stabilization effect was explained by a change in oxygen permeability due to the presence of NPs. Previous studies on HDPE/Cu [18] showed that Cu nanofibers led to a decrease in permeability and therefore protected the material from photodegradation. This phenomenon also appeared to occur at higher Ag NPs loads. The features observed by infrared spectroscopy were corroborated by SEM analysis. While pure polymer and composites with low loads of nanofillers (< 3%) exhibited significant morphological alterations (defects and holes), little or no change was observed for samples containing high amounts (3 and 5 %). Silver nanoparticles inhibited the chain scission process, therefore the thermal properties of the matrix remained almost unchanged. Indeed, DSC analysis showed the photoprotective effect of Ag NPs on HDPE films (the melting point and the degree of crystallinity remained almost constant). In contrast to HDPE, it was shown that the degradation of low-density polyethylene at longer wavelengths triggered the migration of nanoparticles to the surface of the film. As a result, when in contact with water, the material could undergo Ag NPs removal, resulting in a deterioration of the antibacterial properties of the composite materials [19]. It was also reported that UV and thermal ageing caused the brittleness of poly(vinyl chloride)/NPs composite film, which reduced the antibacterial performance of the material. However, despite the migration of NPs to the surface, the percentage reduction of bacteria was close to 99.9 %. This was due to dehydrochlorination of the poly(vinyl chloride). The resulting chlorine atoms would favor the bactericidal capacity [19].

When poly(acrylic acid), PAA, doped with NPs was subjected to polychromatic irradiation at room temperature, a loss of the optical properties of the nanofillers was observed for an exposure time of more than 50 minutes [20]. This behavior was attributed to degradation of the polymeric matrix. Thermogravimetric analysis in an inert atmosphere showed that un-doped and doped PAA, before and after 25 hours of exposure, decomposed into two successive steps. The first one between 200 and 300 °C involved the cleavage of the covalent bonds, responsible for the release of low molecular weight degradation products. The second, between 300 and 500 °C, was related to chain scission reactions and the formation of other degradation species. A decrease in temperature, corresponding to the maximum rate of the first step, was observed for both the PAA/Ag before (about 264 °C) and after irradiation (about 255 °C) compared to un-doped PAA (277 °C initially and 260 °C after 25 hours of irradiation). This result emphasizes the catalytic effect of the nanofiller [20]. This effect was also responsible of the decrease of the nanohardness measured by atomic force microscopy and observed after a few tens of minutes of exposure.

In the case of poly(lactic acid) (PLA), short wavelength irradiation conditions (λ = 254 nm) were quite different from those corresponding to solar irradiation ($\lambda \geq$ 300 nm). However, this study was of crucial importance as UVC light is often used for sterilization and disinfection in medical and pharmaceutical applications [21]. Part of this work was also dedicated to evaluating the influence of Ag NPs (0.2 and 0.5 % loading) on the thermal degradation of PLA at 80 °C [22]. Chemical changes in the macromolecular chain were observed to occur after an induction period that increased with the amount of nanofillers. This was a consequence of the photoprotector effect played by the silver nanoparticles which was associated with an improvement in mechanical properties reported elsewhere [22].

Through the studies described above, it appears that the impact of nanofillers on the stability of polymer/Ag NPs composite material depends greatly on the nature of the

polymeric matrix. Consequently, for the development of new composite materials with new functionalities for applications in different fields, it is difficult to anticipate their behavior under given external stresses. For this reason, the purpose of this present work was to assess how small amounts of silver nanoparticles (0.2 and 0.4 wt.%) dispersed in an acrylate photopolymer could modify the photochemical behavior of the polymeric matrix under the combined effect of light and oxygen. This kind of study necessarily involved a preliminary investigation of the behavior of the pure acrylate polymer under the same experimental conditions, which corresponds to the first part of the present work. The corresponding material was obtained by photopolymerization of a formulation containing poly(ethylene glycol) diacrylate monomer (PEGDA) and pentaerythritoltriacrylate monomer (PETIA). Infrared spectroscopy, differential scanning calorimetry and thermogravimetry were used to monitor the chemical and architectural changes occurring in the corresponding crosslinked polymer. Gas chromatography coupled with mass spectrometry was useful to identify the volatile organic compounds resulting from irradiation and then to develop a mechanism to account for the observed degradation. This kind of approach was successfully applied in previous studies [23, 24]. Once the photodegradation mechanism of the pure polymer matrix was established, the next step was to assess the impact of silver nanoparticles dispersed on the matrix on the degradation process and on the long-term durability of the polymer/Ag NPs nanocomposite.

2. Experimental section

2.1. Materials

Pentaerythritoltriacrylate (PETIA) and poly(ethylene glycol) 600 diacrylate (PEGDA) (Fig. 1) were purchased from Sartomer and used as received without further purification.

a

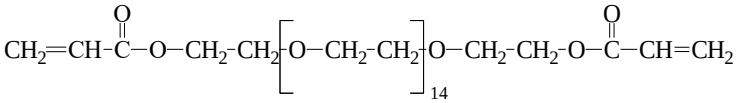

b

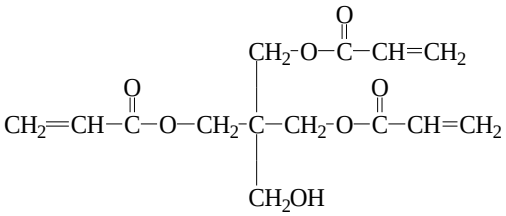

Fig. 1. a) Poly(ethylene glycol) diacrylate (PEGDA) and b) Pentaerythritoltriacrylate (PETIA) monomers.

Silver nitrate ($AgNO_3$, purity > 99%) and the photoinititator 2,4,6-trimethylbenzoyl-diphenyl-phosphineoxide (Darocur®TPO, absorption maximum at 380 nm) were delivered from Aldrich and BASF, respectively.

The typical photopolymerizable formulations were prepared in low-light conditions by mixing the two acrylate monomers (80:20 PEGDA:PETIA) with the photoinitiator (0.5 wt.%). The polymer samples were prepared by coating the photopolymerizable mixture onto a glass slide or a CaF_2 plate (film thickness of 8 ± 1 µm) followed by irradiation using a Xe-Hg source (Lightning cure L8333 with a Hamamatsu L8253 Xe-Hg 100 W lamp). The polymerization was followed by Fourier transformed infrared spectroscopy with the disappearance of the vinyl C=C stretching vibration band at 1410 cm^{-1}.

As regards silver nanocomposite materials, a one-step photo-induced approach was applied [25-28]. Silver nitrate (0.2 or 0.4 wt.%), photoinitiator (0.5 wt.%) and the two acrylate monomers (80:20 PEGDA:PETIA) were stirred under magnetic stirring for one hour at room temperature. This step ensured complete dissolution of the metal precursor and Darocur®TPO, a free radicals generator working through homolytic cleavage of a C-P bond. These highly reactive radicals would be used to reduce silver cations to silver nanoparticles

(Ag NPs). In parallel, these species would also initiate the radical polymerisation of the acrylate monomers. A few drops of the photosensitive formulation were coated onto a glass slide or a CaF_2 plate and then exposed to a fluence of 200 mW cm^{-2} for a few minutes. The formation of silver nanoparticles during the crosslinking polymerization was confirmed by UV-visible spectroscopy (the color of the samples turned to brown-yellow due to the plasmon resonance of silver).

2.2. Experimental set-up and procedure

For photoageing investigations, a SEPAP 12/24 unit from Atlas was used. This ageing simulator device was, in general, equipped with four medium pressure mercury lamps (Novalamp RVC 400 W) located in a vertical position at each corner of the chamber. Wavelengths below 295 nm were filtered off by the glass envelope of the sources. The temperature and the light intensity are parameters that can modify the kinetics of degradation [23,30]. In this work, the SEPAP 12/24 was working with only two lamps (at opposite corners) in order to reduce the light intensity. In the same way, the temperature at the surface of the sample was fixed at 45 °C. A rotating carousel, on which the samples were fixed, was placed at the center of the chamber.

Infrared spectra were recorded on a Nicolet 5SXC FTIR spectrometer with Omnic software. Spectra were obtained with a 4 cm^{-1} resolution and 32 scan summation. UV-visible absorption spectra were recorded on a Shimadzu UV-2600 PC spectrophotometer.

For solid-phase microextraction (SPME) experiments, the photopolymer films (deposited on a glass plate) were irradiated in the SEPAP 12/24 unit, in 20 mL sealed clear glass vials to collect the volatile organic compounds (VOCs) stemming from the photodegradation. Carboxen–PDMS fiber (75 µm) purchased from Supelco (Bellefonte, PA, USA) was used to extract the VOCs in the headspace (HS) [31,32] VOCs were analyzed using SPME coupled

with gas chromatography/mass spectrometry (GC-MS), called HS-SPME/GC-MS, as previously described in details in reference [31]. Mass spectra and reconstructed chromatograms (total ion current, TIC) were acquired under the electron ionization mode (EI) at 70 eV and recorded from 20 to 400 *m/z*. The compounds were identified by comparison with the mass spectra of the spectral library (NIST MS Search Version 2.0).

Thermoporosimetry is a technique that allows the calculation of mesh size distribution from the DSC thermal curve obtained from the freezing of the solvent confined inside the meshes of the polymeric network [33-36]. In this study the solvent was deionized water. DSC analysis was carried out with a Mettler Toledo DSC 3+, with cooling from 5°C to -85 °C at rate of 0.7 °C min^{-1}. Analyses were performed on swelled films for four weeks, which were placed in a 100 µL aluminum crucible.

The mesh size distribution $\frac{dV_P}{dR_P}$ as a function of the mesh radius R_P, where the phase transition occurred, was calculated from the relationship $\frac{dV_P}{dR_P} = \frac{kY(T)\Delta T^2}{18.8 W_a R_P}$. V_P was the mesh volume, Y(T) was the DSC thermal curve ordinate corrected by the baseline. k designed a proportionality coefficient that depended on the rate of cooling and the sensitivity of DSC instrument. W_a was the apparent enthalpy of crystallization of water that verified an empirical equation established by calibration in a previous work [36]. ΔT was the difference in the crystallization temperatures of the confined and the free water. The different steps followed to calculate the mesh size distribution $\frac{dV_P}{dR_P} = f(R_P)$ from DSC thermogram was described in detail in reference 36.

DSC-TGA curves were recording using SetSys Evolution 1750 – SETARAM at temperatures ranging from 25 °C to 500 °C with a heating rate of 5 °C min^{-1}.

Transmission electron microscopy (TEM) measurements were achieved at 200 kV employing a Philips CM200 instrument with LaB6 cathode in order to observe morphology and in-depth organization of Ag NPs inside the polymer matrix. For the analysis, samples were cut with an ultra-microtome and observed on their cross sections.

3. Results and discussion

3.1. Photochemical behavior of the pure acrylate polymer

3.1.1. Chemical modifications

Under accelerated photoaging, pure PEGDA/PETIA polymer (deposit on a CaF_2 plate, thickness ca 8 µm) underwent chemical modifications as shown by the infrared spectra, recorded at various increasing exposure times (Fig. 2a).

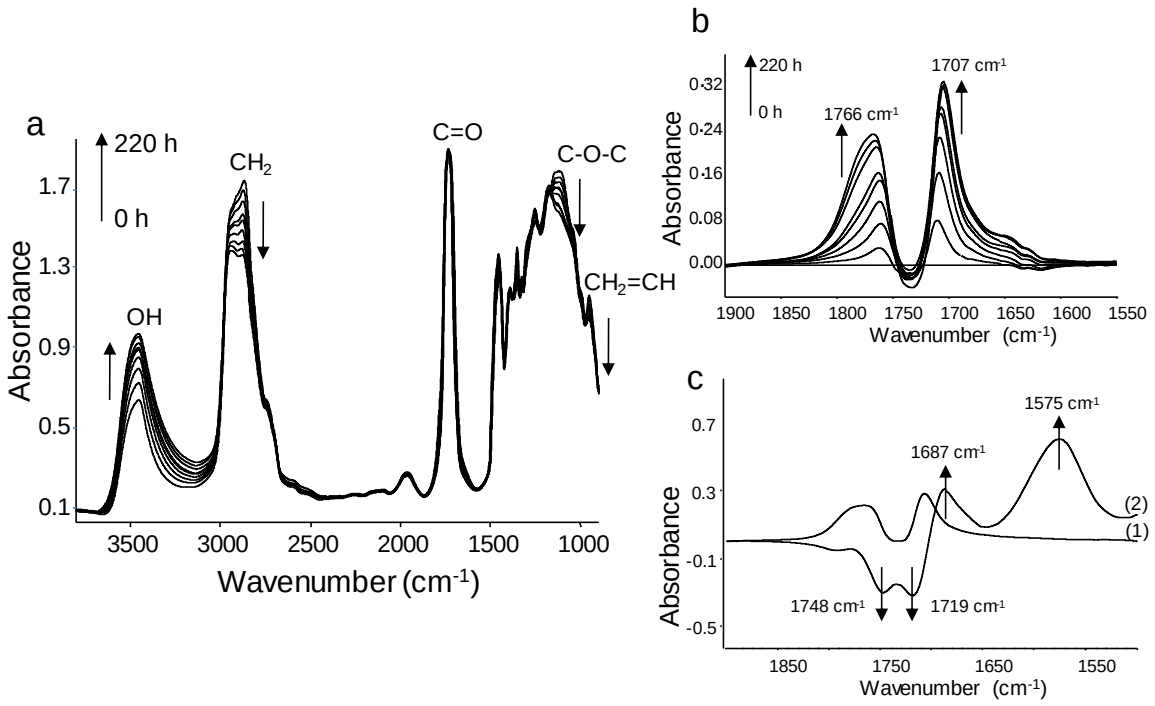

Fig. 2. a) Changes in infrared spectra of film of pure PEGDA/PETIA upon irradiation in SEPAP 12/24 at 45 °C. b) Evolution of the differential infrared spectra of pure polymer

(subtraction between spectra after and before irradiation) in the carbonyl domain upon irradiation. c) Differential infrared spectra (1) of irradiated film – unirradiated film and (2) of irradiated film after NH_3 treatment – irradiated film before treatment.

Two phenomena simultaneously occurred. The first one was a post-polymerization that consumed the residual vinyl groups (band at 951 cm^{-1}, Fig. 2a). Such reaction was already observed in acrylate photopolymers [23]. The second process was the photooxidation of the polymeric matrix. Irradiation caused the decrease of the bands at 2871 and 1115 cm^{-1} related to the methylenic and ether groups of PEG units, respectively. The absorbances of these two bands were linearly correlated (not shown). At the same time, new hydroxyl groups (increase of absorbance of the OH bond vibration band centered at 3460 cm^{-1}) and carbonyl functions were formed. In the carbonyl domain (1900-1500 cm^{-1}), the evolution of the differential infrared spectra (subtraction between the infrared spectra after and before irradiation) showed an increase in absorbance around 1707 and 1766 cm^{-1}, unfortunately the maxima of the corresponding bands were not observed due to the large band of the initial ester groups at 1735 cm^{-1}. (Fig. 2b). At this stage, it was important to note that previous studies carried out on poly(ethylene oxide) have shown that under accelerated conditions, the ether groups were favorable sites for oxidative degradation and therefore unstable [23,37-38]. These studies evidenced the fact that the combination of light exposure and oxygen resulted in the formation of formate (band at 1725 cm^{-1}) and ester (band at 1750 cm^{-1}) groups. In order to identify the resulting photoproducts, an irradiated PEGDA/PETIA film was exposed to NH_3. The aim of this derivatization treatment was to evidence the formation of acid and ester functions. After the treatment, acid functions convert into carboxylate groups, ester into amide groups [39] and formate end group into formamide [37]. Differential spectra (subtraction between the spectra after and before treatment, Fig. 2c) revealed the band decrease at 1719 and 1748 cm^{-1} and in parallel, the band formation at 1575 cm^{-1} (carboxylate) and 1687 cm^{-1} (amide derived from

esters and formates). Subsequently, the evolution of esters during ageing was followed by an increase in absorbance at 1766 cm^{-1}.

Changes in the chemical structure of the copolymer were mainly the result of chain scission reactions that were accompanied by the consumption of the methylene groups. As a result of these reactions, low molecular weight compounds might have evolved. In order to obtain information on the resulting gases, HS-SPME/GC-MS was used. This technique is a very powerful tool for monitoring polymer degradation and determining the mechanism of their photo-oxidation [23,24,40-42]. It was applied to samples irradiated for 0, 3, 10, 26, 50 and 100 hours. As an illustration, Fig. 3 displays the chromatogram of a film irradiated 50 hours. It highlights the migration of various low molecular weight compounds into the gas phase.

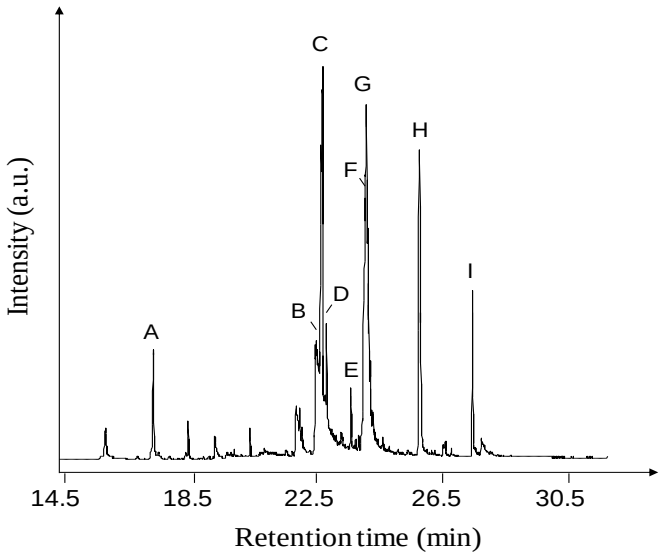

Fig. 3. TIC HS-SPME/GC-MS chromatogram of a PEGDA/PETIA film irradiated 50h in a SEPAP 12/24 ($\lambda \geq 300$ nm, 45 °C).

All the compounds were identified (Table 1). According to M.N. Mortensen [43], formic acid (compound B) detected at 22.4 minutes resulted from hydration of formate resulting from the photo-oxydation of PEG units. To account for these gases, some degradation pathways are proposed in Figures 4 to 6. Based on the decay of methylene groups and –C-O-C bonds,

revealed by infrared spectroscopy, the photo-oxidation of PEG units could involve abstraction of labile hydrogens in α position to oxygen atom.

Table 1. Volatile organic compounds stemming from irradiated PEGDA/PETIA film as identified by HS-SPME/GC-MS.

Retention time (min)	Products
16.9	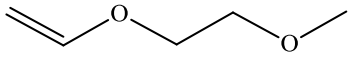 (2-methoxyethoxy)ethene (A)
22.4	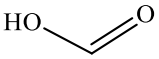 Formic acid (B)
22.6	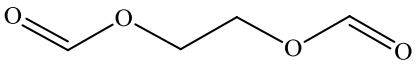 Ethylene glycol diformate (C)
22.8	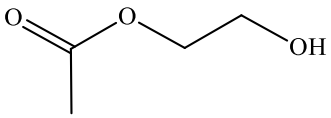 2-hydroxyethyl acetate (D)
23.6	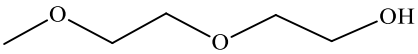 (2-methoxyethoxy)ethanol (E)
24.1	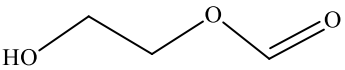 2-hydroxyethyl formate (F)
24.2	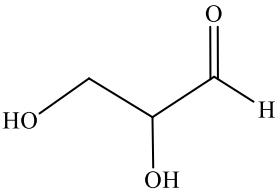 2,3-dihydroxypropanal(G)
25.9	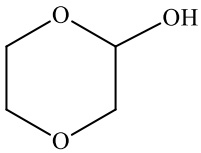 1,4-dioxan-2-ol (H)
27.7	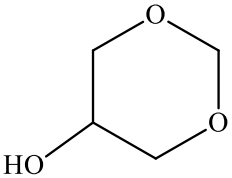 1,3-dioxan-5-ol (I)

At this step, it should be mentioned that, based on previous studies on photopolymers synthesized from the polymerization of 2(2-ethoxy ethoxy)ethyl acrylate, HS-SPME/GC-MS analysis also evidenced the formation of ethylene glycol diformate (compound C detected at

22.6 min) stemming from the photo-oxidation. A mechanism was proposed to account for the release of this low molecular weight compound [23]. By analogy, mechanistic hypothesis was ventured to explain the formation of this species (Fig. 4).

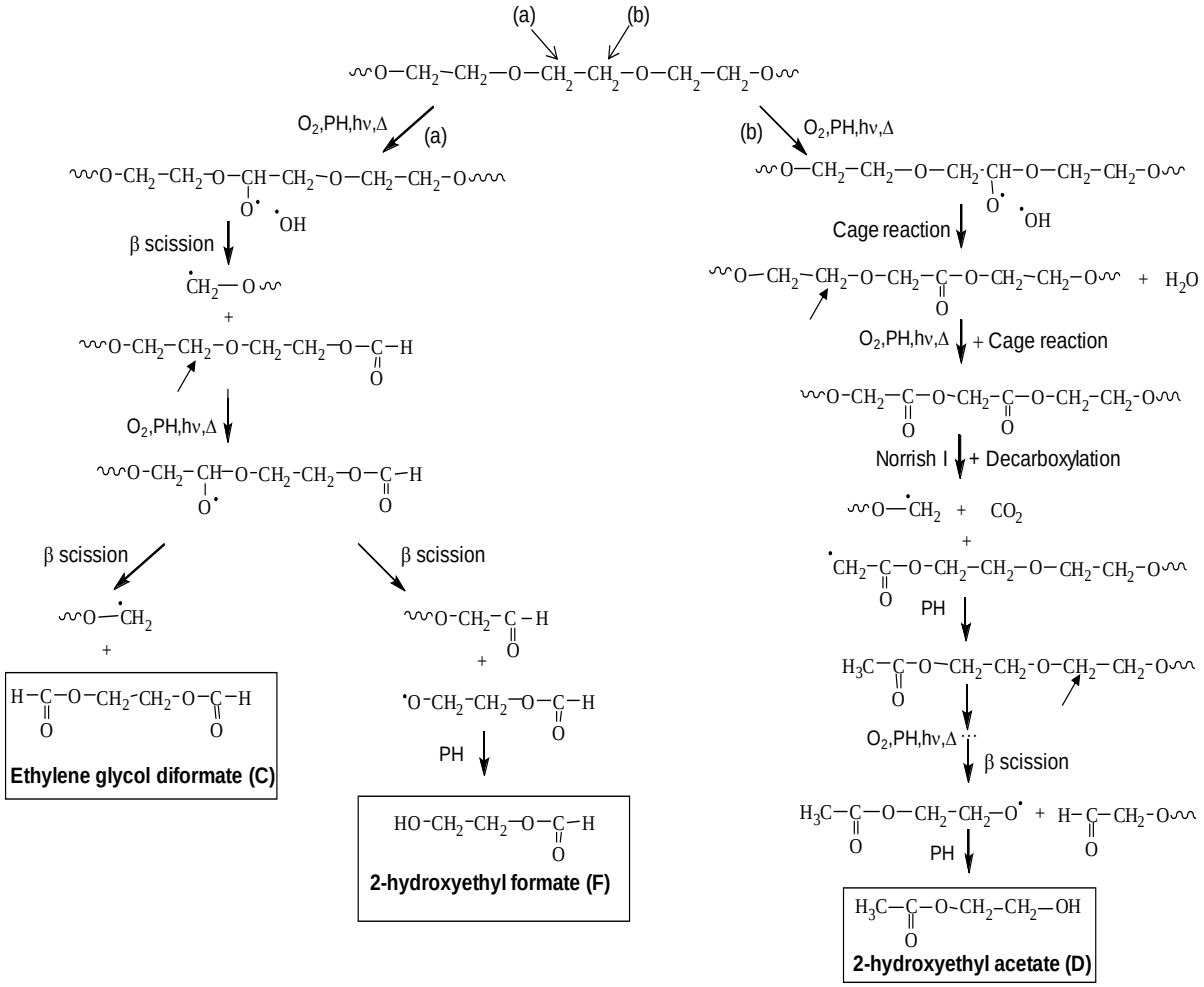

Fig. 4. Proposed mechanism of formation of ethylene glycol diformate, 2-hydroxyethyl formate and 2-hydroxyethyl acetate from oxidative degradation of PEGDA/PETIA initiated by H abstraction at positions (a) and (b). PH designs the polymer.

Hydrogen abstraction in α position to oxygen atom could occur either at position (a) or (b). Alkoxy radicals derived from route (a) through hydroperoxide formation could undergo a β scission reaction that led to monoformate end groups carried by side polymer chains. After H abstraction and β scission reaction, this latter could give rise either to ethylene glycol

diformate (compound C) or 2-hydroxyethyl formate (compound F) (Figure 4). β-scission reaction not only yielded compound F but also aldehyde end groups, which could in turn oxidize into acid. This was consistent with infrared spectroscopy which revealed the presence of carboxylic acid in the polymer chain upon exposure, a result confirmed as indicated above, by the NH_3 treatment.

A mechanism of photo-oxidation initiated by Norrish I and/or ester elimination reactions then followed by decarboxylation and/or decarbonylation [44,45] was proposed to rationalize the results obtained in a previous study on the photostability of acrylate photopolymer (Fig. 4 in reference 23). The $^{\bullet}O\text{-}CH_2CH_2\text{-}O$- and $^{\bullet}CH_2\text{-}O\text{-}CH_2CH_2\text{-}O$- radicals generated from the two chain scission processes could account for the formation of compounds A, E, G and H. (2-methoxyethoxy)ethanol arose from hydrogen abstraction in α position to methylene groups of macroalkoxyradicals $^{\bullet}O\text{-}CH_2CH_2\text{-}O$- and then from β scission (Fig. 5). Compound H might be the result of two successive H abstractions in α position to CH_2 groups in the same macromolecular chain giving rise to alcohol and ester functions. The resulting compound would in turn undergo chain scission by Norrish I or ester elimination reaction followed by decarboxylation process. The resulting biradical would yield 1,4-dioxan-2-ol after intramolecular recombination.

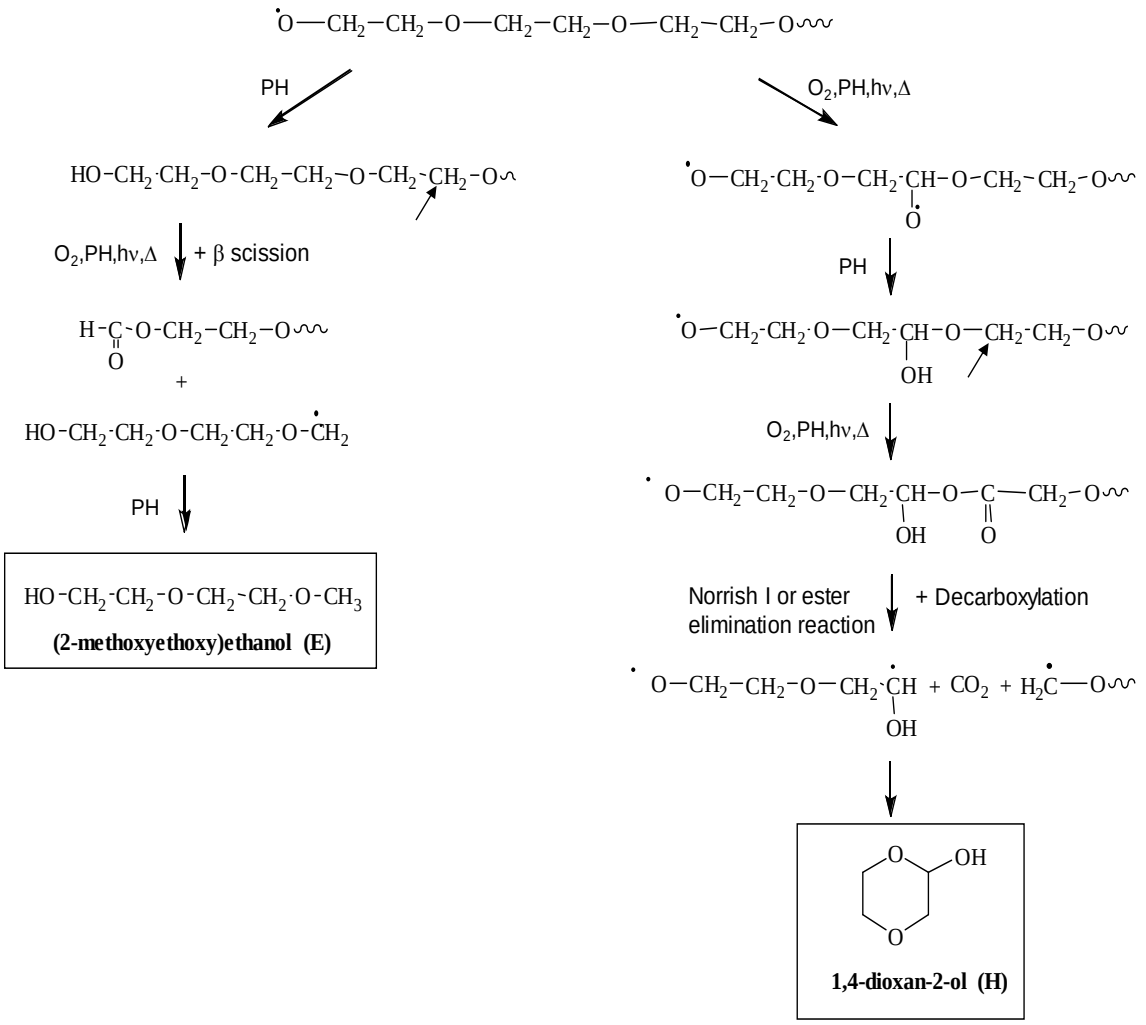

Fig. 5. Proposed degradation pathways of macroalkoxy radicals derived from Norrish I cleavage and/or ester elimination reaction degradation of PEGDA/PETIA polymer.

The degradation pathway of the polymer initiated by H abstraction at position (b) in the mechanism displayed in Fig. 4 might explain the formation of 2-hydroxyethyl acetate through successive reactions: cage reaction, oxidation, Norrish I cleavage giving rise $^{\bullet}CH_2$-COO-CH_2-CH_2-O- radicals. This latter would in turn convert into 2-hydroxyethyl acetate according to the mechanism shown in Fig. 4.

A mechanism accounting for the formation of 2,3-dihydroxypropanal and (2-methoxyethoxy)ethene was proposed in Fig. 6.

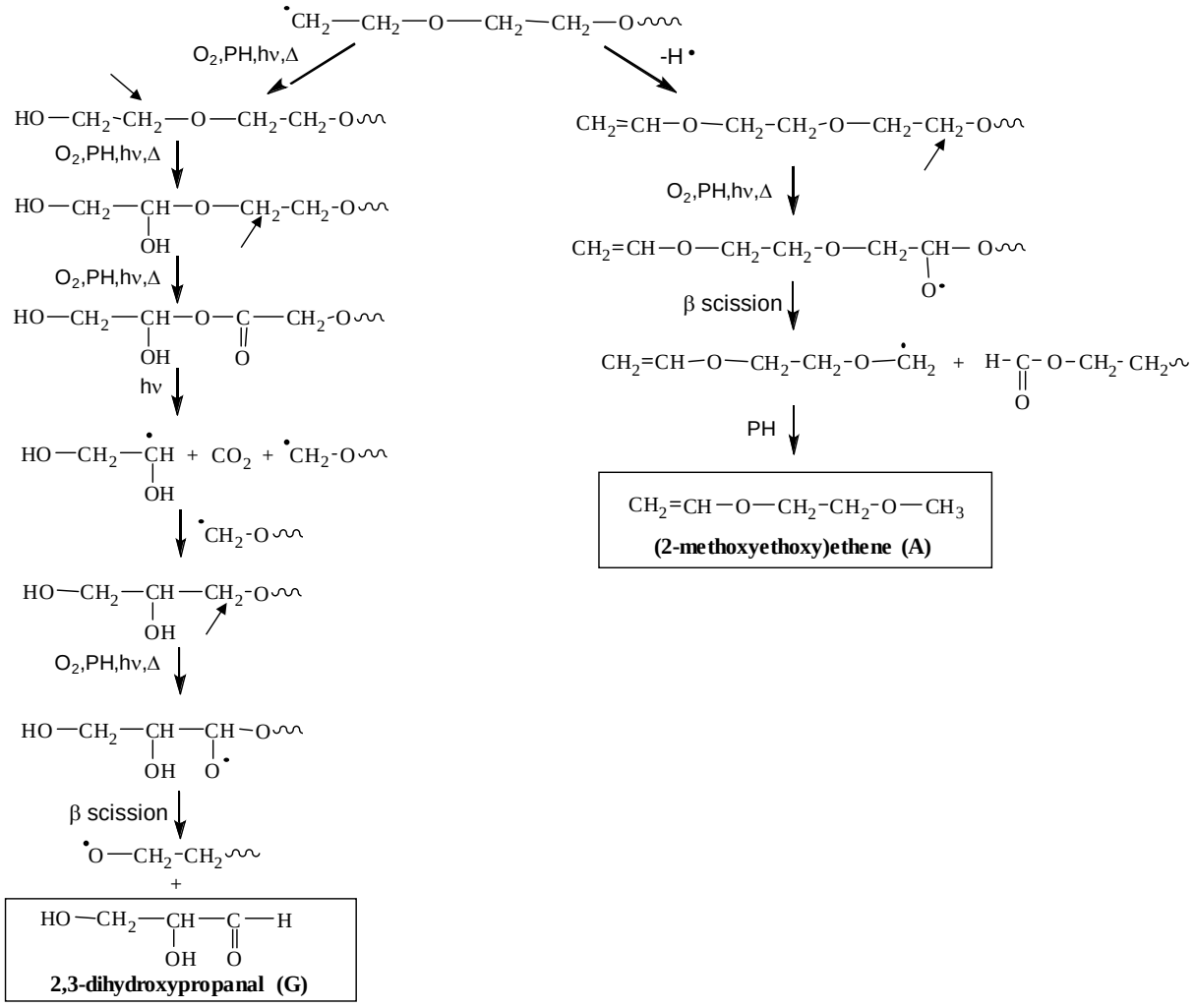

Fig. 6. Proposed degradation pathways of macroalkyl radicals resulting from Norrish I cleavage and/or ester elimination reaction degradation of PEGDA/PETIA polymer.

2,3-dihydroxypropanal was the result of successive oxidation reactions involving various attack sites of $^{\bullet}CH_2$-CH_2-O- macroradicals and radical re-combinations involving $^{\bullet}CH_2$-O- radicals, followed by H abstraction in α position to the oxygen atom of the ether groups. According to M.N. Mortensen [43], the double bond of (2-methoxyethoxy)ethene species arose from $H^{\bullet}$ radical. The oxidation of the methylene group gave rise to alkoxy radicals that yielded another radical through β scission. This latter would then convert into (2-methoxyethoxy)ethene (compound A), which was detected at 16.9 minutes (Fig. 6).

Taking into account the surface area of the HS-SPME/GC-MS peaks, it appears that regardless of the irradiation time, ethylene glycol diformate (compound C) remained the main

gas released (Fig. 7). Similarly, 2-hydroxy ethyl formate (compound F) and 2,3-dihydroxypropanal (compound G) were formed at a high concentration, but at a lower concentration than compound C. These characteristics could suggest that H abstraction at position (a) proposed as initiation step of degradation pathway in Fig. 4 could be the major degradation pathway for PEGDA/PETIA polymer. Thus, pathway (b) did not appear to be a preponderant pathway (Fig. 4). The proposed mechanism to explain the formation of 2,3-dihydroxypropanal derived from $^{\bullet}CH_2$-O-CH_2CH_2-O- radicals could also be considered as one of the major degradation pathways (Fig. 6)

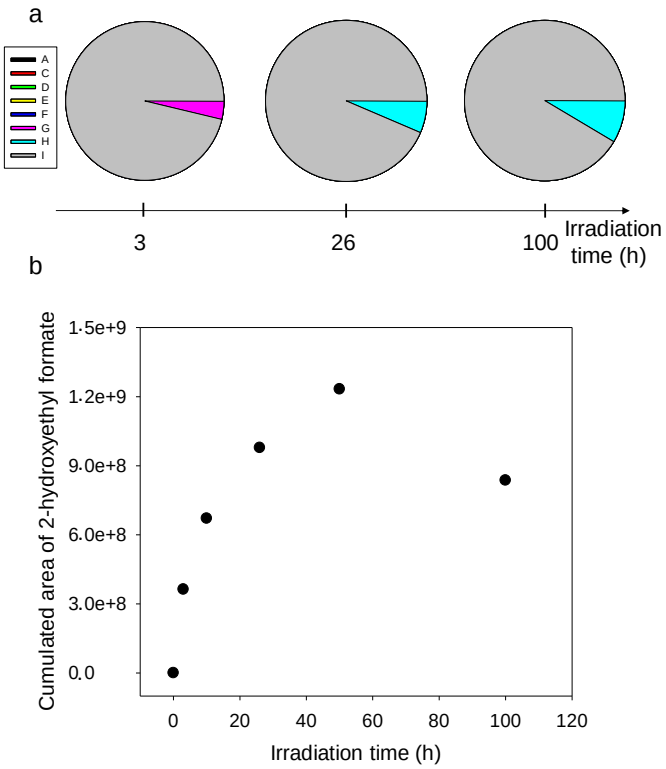

Fig. 7. a) Distribution, by cumulated area, of volatile organic compounds (from compound A to I except compound B) stemming from PEGDA/PETIA films irradiated 3, 26 and 100 h in SEPAP 12/24 ($\lambda \geq$ 300 nm, 45 °C). b) Kinetics evolution of formation of 2-hydroxy ethyl formate (compound F detected at 24.1 minutes).

Concerning 2-hydroxy ethyl formate, its concentration increased, went through a maximum at 50 hours of exposure and then decreased (Fig. 7b). Such a behavior could be explained by a conversion of this compound into formic acid [43].

3.1.2. Thermal analysis

Photoageing causes the polymer to undergo chain scission reactions that should have an impact on the size of the meshes of the three-dimensional network. To highlight this, we used thermoporosimetry which is a powerful technique to monitor the distribution of mesh size from the DSC thermogram during irradiation. Prior to exposure, water was trapped in meshes with radius ranging from 1.63 to 1.9 nm (Fig. 8). After 3 hours, the average mesh size distribution shifted to a higher R_P from 2.8 to 4.8 nm. This result highlighted that at earlier exposure time, polymer degradation was sufficient to increase the mesh size. This increase occurred despite the post polymerization that took place in parallel with the degradation process. After 10 hours, the mesh radius was between 2.1 and 4.1 nm. It is interesting to mention that DSC thermograms of samples irradiated 26 and 50 hours, only displayed the crystallization peak of free water. This could be the result of important chain scission reactions occurring in the polymer which were responsible for the non-confinement of the solvent (the mesh sizes were too large).

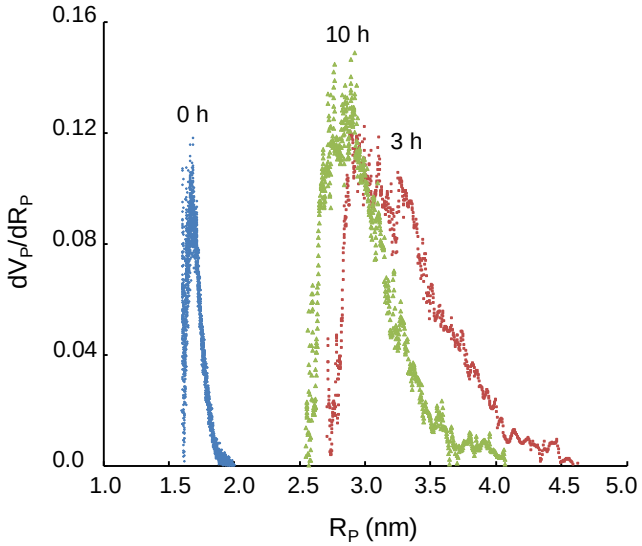

Fig. 8. Mesh size distribution of a film of PEGDA/PETIA before and after 3 and 10 hours of irradiation in SEPAP 12/24 ($\lambda \geq 300$ nm, 45 °C).

As regards the thermal properties of the copolymer, before irradiation, DSC thermogram showed three peaks with maxima at 180, 270 and 370 °C. After 3 hours of exposure, the second peak disappeared. Changing the composition of the monomer mixture did not allow us to attempt this peak. This could be related to residual monomer or unreacted functions that are converted during the first three hours of photoageing, as a post-polymerization phenomenon.

To obtain information on the influence of photoageing on thermal properties of the polymer at higher temperatures, thermogravimetric analyses coupled with DSC were performed on samples irradiated 3 and 10 hours in SEPAP 12/24 and at 45 °C. The thermal parameters obtained are presented in Table 2.

Table 2. Thermal parameters of PEGDA/PETIA film before and after 3 and 10 hours of irradiation in SEPAP 12/24($\lambda \geq$ 300 nm, 45 °C).

	Peak 1		Peak 2		Peak 3	
	$T_{decomposition}$	Δm (%)	$T_{decomposition}$	Δm (%)	$T_{decomposition}$	Δm (%)
0 h	112-221	8	222-317	45	317-423	30
3h	108-293	44			293-434	41
10h	103-288	50			288-421	37

Temperatures in °C

The decomposition of irradiated PEGDA/PETIA films occurred in two steps: the first in the 103-293 °C range and the second at 288-421 °C. These steps were also observed in thermogravimetric analysis of poly(acrylic acid) [20]. By analogy, the first step might be attributed to the cleavage of the covalent bonds. The corresponding weight loss was 44 % and 50 % after 3 and 10 hours of irradiation, respectively, compared to the low value of 8 % obtained for the unirradiated polymer film. As regards the last peak, it might be related to a chain scission reaction. Exposure resulted in a small increase in weight loss from 30 % before irradiation to 40 % and 37 % after 3 and 6 hours of photoageing, respectively (Table 2).

3.2. Influence of silver nanoparticles on the photochemical behaviour of the polymeric matrix

The influence of ageing on 0.2% and 0.4% silver filled samples was first evaluated by UV-visible spectroscopy (Fig. 9a). Absorbance spectra show that ageing induced an increase of the plasmon band with a small shift from 416 nm to 425 nm for both concentrations. During the first 50 hours of photoageing, the plasmon band progressively shifted to red, from 416 nm (without aging) to 420 nm (10 h) and finally to 425 nm (50 h) which indicated a small

coalescence of the NPs in both concentrations. Between 50 and 100 h no more evolution was observed in terms of wavelength shift, no more coalescence. In the same time, the intensity on the plasmon increased progressively in both concentration (Fig. 9b), behavior ascribed to the reduction of residual silver ions. No evolution of the UV-visible spectra between 200 to 600 nm was observed for the polymer without NPs.

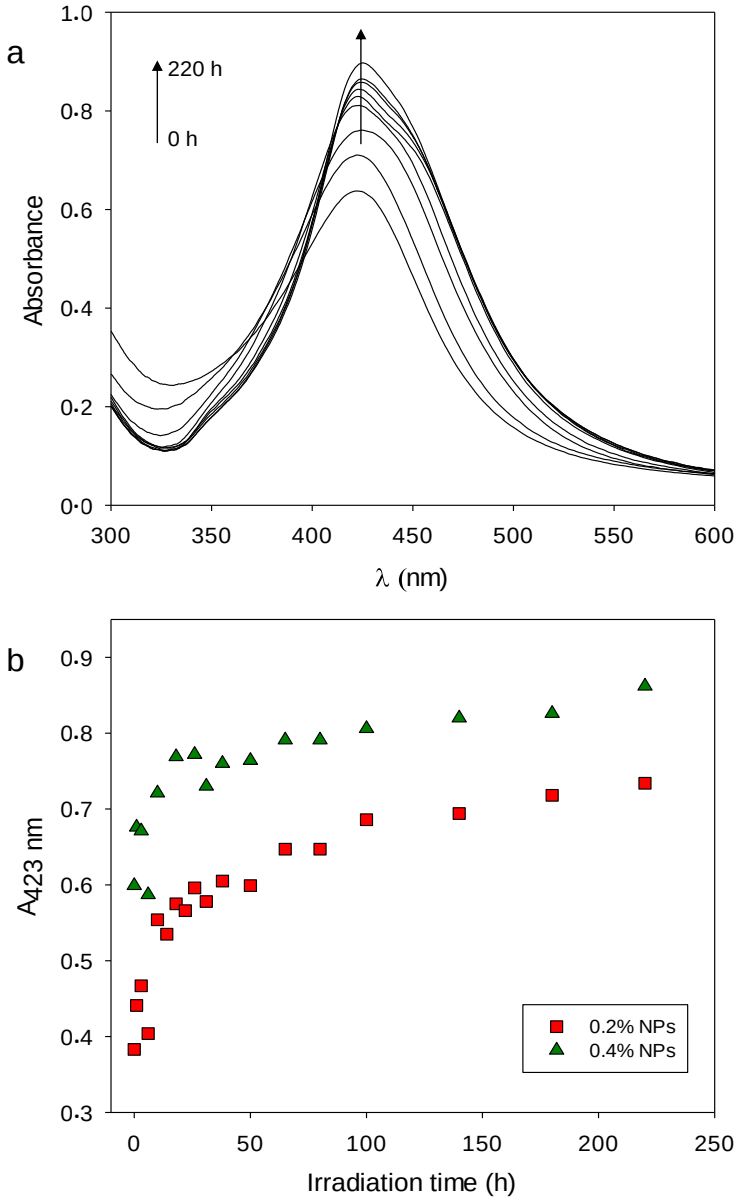

Fig. 9. a) Evolution of UV-visible spectra of the surface plasmon band of Ag NPs dispersed in PEGDA/PETIA polymer film (0.4% of NPs) upon irradiation. b) Kinetic evolution of the surface plasmon band at 423 nm during photoageing of composite materials.

TEM characterizations of sample cross sections were realized to visualize the changes of silver nanoparticles in terms of size/shape and organization in the polymer matrix (Figure 10). Before ageing, the particles were homogeneously dispersed in the matrix for both concentrations. The size distribution was bigger at 0.4 % of AgNPs (3 to 15 nm) than 0.2 % (1.5 to 5 nm). After 100 hours of exposure, particles size slightly increased and a clear structuring of the nanoparticles was observed with a depth wise gradient of nanoparticles concentration toward the air surface of the nanocomposite film (Fig. 10). These changes resulted from migration and coalescence of the silver nanoparticles to the air surface of the nanocomposite film, phenomena also occurred in poly(vinyl chloride)/NPs composite film during UV and thermal ageing, and in low-density polyethylene/NPs material at longer wavelengths exposure [19]. The migration phenomenon was also observed by Tenorio-Neto et al. after 1 hour of a thermal treatment at 180°C of copolymer/Ag NPs nanocomposite [46].

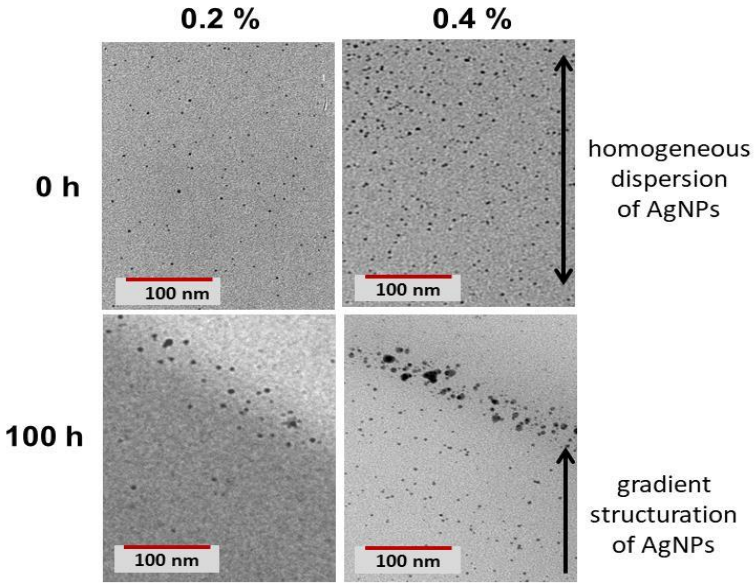

Fig. 10. TEM images of samples cross section before and after 100 hours of exposure in SEPAP 12/24 (λ≥ 300 nm, 45 °C) for both concentrations of Ag NPs (0.2 and 0.4%).

The chemical changes in the polymeric matrix followed by infrared spectroscopy were identical to those observed during the photo-oxidative degradation of the pure copolymer. To try to better establish the role played by silver nanoparticles in both photo-oxidation and post-polymerization processes, it is necessary to investigate the kinetic aspects of these processes. Fig. 11a revealed that the higher the amounts of NPs, the greater the decay of the methylene groups. Indeed, for example after 220 hours of irradiation in the case of un-doped polymer, 25 % of CH_2 were consumed compared to 39 and 65 % when 0.2 and 0.4 % of NPs were dispersed in the polymer matrix, respectively. Such results highlighted the photocatalytic effect played by nanofillers even used in low quantity. This effect was also observed in the case of HDPE/Ag NPs composite when the load of NPs was lower than 3%. On contrary for amounts superior to 3%, the nanofillers could avoid chain scission reactions to occur and finally act as a protector role [17]. Thus, in PEGDA/PETIA matrix both concentrations of Ag NPs favored the chain scission phenomenon that caused the migration of the nanoparticles upon ageing, also reported in low-density polyethylene/Ag NPs composite [19].

The influence of Ag NPs was also evidenced in the kinetics of formation of new ester groups followed by infrared spectroscopy at 1766 cm^{-1} (Fig. 11b). Fig. 11b showed that the concentration of this species increased with increasing amounts of NPs. Interestingly, a linear correlation between the formation of ester groups and the decay of CH_2 groups was observed regardless of the NPs loading in the nanocomposite (0, 0.2 and 0.4 %).

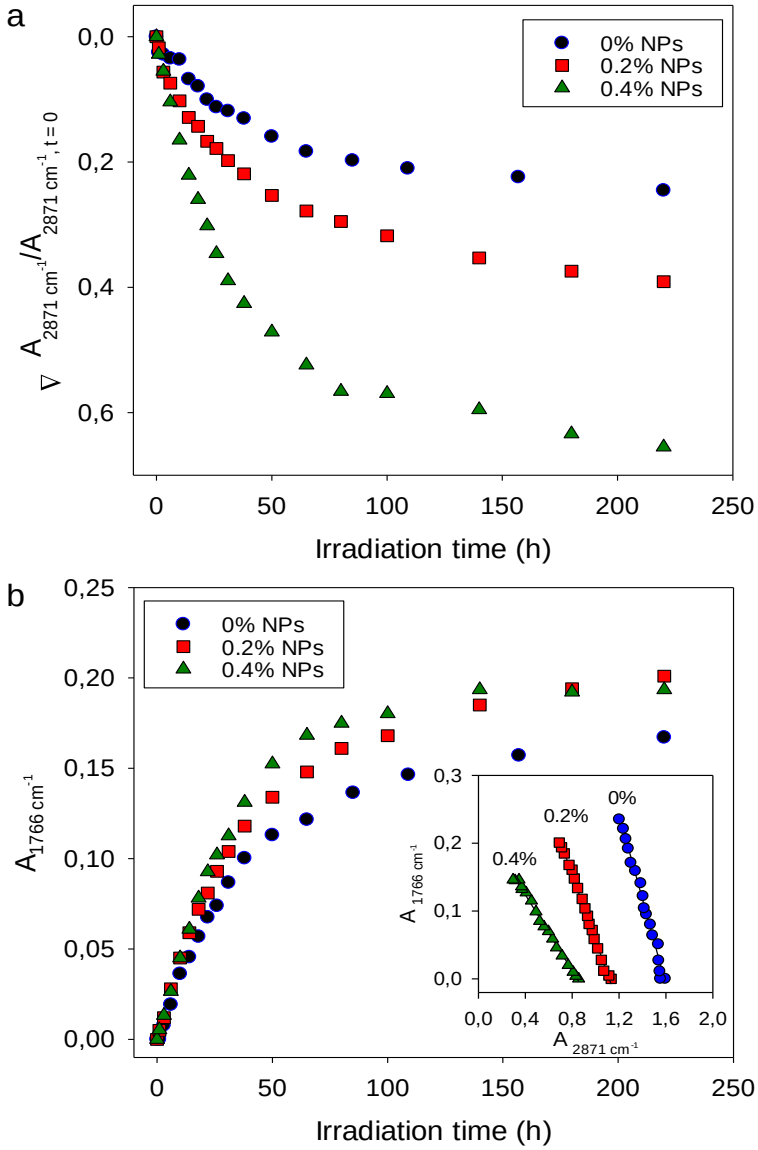

Fig. 11. Comparison of kinetic evolution of a) the decay of methylene groups (band at 2871 cm^{-1}) and b) the formation of ester groups (band at 1766 cm^{-1}) for the pure and Ag NPs dispersed PEGDA/PETIA polymer (0.2 and 0.4 % of NPs) upon irradiation. Inset: Correlation between the band at 2871 cm^{-1} (CH_2 groups) and the band at 1766 cm^{-1} (ester groups) of pure and doped polymer.

Silver nanoparticles not only modified the kinetics of photodegradation but also the kinetics of the post-polymerization reaction. As an example, in the case of composite with 0.4 % filler, the percentage decrease in residual vinyl groups was 73 % after 65 hours of

irradiation compared to 10 % in the case of an unfilled polymer. According to the literature [27], the polymerization process was initiated by the silver nanofiller and thus, addition of Ag^+ ions to the photopolymerizable formulation increased the ultimate conversion degree of acrylate groups. The obtained results were in agreement with the literature.

After the absorption of photons, an electron-hole pair was photogenerated and could react with water and O_2 molecules [12]. As a result, hydroxyl radicals were formed. It is known that this species are the main reagents in the photocatalytic process; they can promote hydrogen abstraction and thus initiate the degradation phenomenon. Thus, the higher the amount of Ag NPs in the polymer, the higher the concentration of hydroxyl radicals and finally the more important the photocatalytic effect, as revealed in Fig. 11a and 11b.

Conclusion

In this study, we were interested in new acrylate photopolymers containing Ag NPs. The development of these new classes of composites depends crucially on their ability to resist photoageing over a long period of time.

Thus, to assess this point, our work was first devoted to the photostability of the un-doped polymer matrix. In an environment simulating sunlight, a post-polymerization of residual vinyl groups and an oxidation developed in this material. The latter process led to chemical changes (degradation of the $-CH_2CH_2-O-$ groups of the PEGDA units and formation of new carbonyl functions on the polymer backbone) and architectural modification (increase in pore size). The chain scission responsible of the instability of PEG units caused, as expected, the formation of volatile organic compounds identified by SPME/GC-MS.

In the second part of this work, the influence of addition of low amount of Ag NPs (0.2 and 0.4 % loading) on post-polymerization and photo-oxidation kinetics was examined. NPs promoted the polymerization of the residual vinyl groups. However, the investigation

highlighted the photocatalytic effect played by nanoparticles involving hydroxyl radicals resulting from the reaction between absorbed water and photogenerated electron-hole pairs. This means that silver nanoparticles unfortunately had an impact on the durability of the polymer matrix and therefore of the composite material. This unwanted characteristic is all the more important as these nanocomposite materials could find great applications in textile industry thanks to the specific properties of silver nanofillers (antibacterial, optical, conductive properties). Besides, under irradiation, Ag NPs underwent size distribution modification and a gradient structuring as a result of migration to the surface of the film and coalescence.

Very recently materials with reflective metallic top coatings and with spatially control of the assembling process of Ag NPs in a 3D polymer network have been developed. Since silver nanofillers have a rather negative effect on the photostability of the composite material, the question arises whether the reflective metallic top coating might not, on the contrary, provide some form of protection of the polymer matrix against degradation. This will be the subject of a forthcoming study focusing on the photostability of these nanocomposite materials specially designed to open up new perspectives in the textile industry.

Acknowledgements

The authors thank the Agence Nationale de la Recherche (ANR) for financial support under contract ANR-16-CE08-0032-01 projet MeTex.

Lawrence Frezet is thanked for his help in recording DSC-TGA curves.

References

[1] A. G. Koniuszewska, J. W. Kaczmar, Application of polymer based composite materials in transportation, Progess in Ruber, Plastics and Recycling technology 32 (2016) 1-23.

[2] B. Harris, A perspective view of composite materials development, Materials & Design 12 (1991) 259-272.

[3] A. J. Haes, D. A. Stuart, S. Nie, R.P. van Duyne, Using solution-phase nanoparticles, surface-confined nanoparticle arrays and single nanoparticles as biological sensing platforms, J. Fluoresc. 14 (2004) 355-367.

[4] M. Pumera, Graphene in biosensing, Mater. Today 14 (2011) 308-315.

[5] K. Chaloupka, Y. Malam, A.M. Seifalian, Nanosilver as a new generation of nanoproduct in biomedical applications, Trends Biotech. 28 (2010) 580-588.

[6] L. Guo, W. Yuan, Z. Lu, C.M. Li, Polymer/nanosilver composite coatings for antibacterial applications, Colloids and Surfaces A: Physicochem. Eng. Aspects 439 (2013) 69-83.

[7] P. Dallas, V.K. Sharma, R. Zboril, Silver polymeric nanocomposites as advanced antimicrobial agents: Classification, synthetic paths, applications, and perspectives, Adv. Colloid Interface Sci. 166 (2011) 119-135.

[8] D.D. Evanoff Jr., G. Chumanov, Synthesis and optical properties of silver nanoparticles and arrays, ChemPhysChem 6 (2005) 1221-1231.

[9] M. Diantoro, T. Suprayogi, U. Sa'adah, N. Mufti, A. Fuad, A. Hidayat, H. Nur, Modification of electrical properties of silver nanoparticle, IntechOpen (2018) 233-248. http://dx.doi.org/10.5772/intechopen.75682

[10] K. Gupta, P.C. Jana, A.K. Meikap, Optical and electrical transport properties of polyaniline-silver nanocomposite, Synthetic Metals 160 (2010) 1566-1573.

[11] K. Roy, C.K. Sarkar, C.K. Ghosh, Photocatalytic activity of biogenic silver nanoparticles synthesized using yeast (Saccharomyces cerevisiae) extract, Appl. Nanosci. 5 (2015) 953-959.

[12] M.S. Punnoose, B. Mathew, Treatment of water effluents using silver nanoparticles, Mater. Sc. Eng. 2 (2018) 159-166.

[13] E.E. Elemike, D.C. Onwudiwe, A.C. Ekennia, R.C. Ehiri, N.J. Nnaji, Phytosynthesis of silver nanoparticles using aqueous leaf extracts of Lippia citriodora: Antimicrobial, larvicidal and photocatalytic evaluations, Mater. Sci. Eng. C 75 (2017) 980-989.

[14] M. Kumari, N. Thapa, N. Gupta, A. Kumar, S. Nimesh, Antibacterial and photocatalytic degradation efficacy of silver nanoparticles biosynthesized using Cordia dichotoma leaf extract, Adv. Nat. Sci.: Nanosci. Nanotechnol. 7 (2016) 045009-0450016.

[15] S. Francis, K.M. Nair, N. Paul, E.P. Koshy, B. Mathew, Catalytic activities of green synthesized silver and gold nanoparticles, Materials Today: Proceedings 9 (2019) 97-104.

[16] S. Nahar, M.R. Hasan, A.A.H. Kadhum, H.A. Hasan, M.F.M. Zain, Photocatalytic degradation of organic pollutants over visible light active plasmonic Ag nanoparticle loaded Ag_2SO_3 photocatalysts, J. Photochem. Photobiol. A: Chemistry 375 (2019) 191-200.

[17] I. Grigoriadou, E. Pavlidou, K.M. Paraskevopoulos, Z. Terzopoulou, D.N. Bikiaris, Comparative study of the photochemical stability of HDPE/Ag composites, Polym. Degrad. Stab. 153 (2018) 23-36.

[18] I. Grigoriadou, K.M. Paraskevopoulos, M. Karavasili, G. Karagiannis, A. Vasileiou, D. Bikiaris, HDPE/Cu-nanofiber nanocomposites with enhanced mechanical and UV stability properties, Comp. B. Eng. 55 (2013) 407-420.

[19] R. Chinkamonthong, A. Kositchaiyong, N. Sombatsompop, Effects of thermal and UV aging on antibacterial properties of linear low-density polyethylene and poly(vinyl

chloride) films containing nano-silver colloid, Journal of Plastic Film & Sheeting 29 (2012) 144-162.

[20] H. Kaczmarek, M. Metzler, K.Wegrzynowska-Drzymalska, Effect of stabilizer type on the physicochemical properties of poly(acrylic acid)/silver nanocomposites for biomedical applications, Polym. Bull. 73 (2016) 2927-2945.

[21] M. Mucha, S. Bialas, H. Kaczmarek, Effect of nanosilver on the photodegradation of poly(lactic acid), J. Appl. Polym. Sci. 131 (2014) 40144-40151.

[22] M. Mucha, S. Ksiazek, Comparison of photochemical and thermal degradation of poly(lactic acid) doped by nanosilver, J. Chem. Chem. Eng. 9 (2015) 23-30.

[23] G.G. Goourey, P. Wong-Wah-Chung, F. Delort-Jestin, B. Legret, L. Balan, Y. Israëli, Photostability of acrylate photopolymers used as components in recording materials, Polym. Degrad. Stab. 119 (2015) 208-2016.

[24] G.G. Goourey, P. Wong-Wah-Chung, L. Balan, Y. Israëli, Influence of ZnO nanoparticles in the photostability of acrylate photopolymers used as components in recording materials, Polym. Degrad. Stab. 153 (2018) 172-184.

[25] G. Mustatea, I. Calinescu, A. Diacon, L. Balan, Photoinduced synthesis of silver/polymer nanocomposites, Materiale Plastice 51 (2014) 17-21.

[26] M. Sakamoto, M. Fujitsuka, T. Majima, Light as a construction tool of metal nanoparticles: synthesis and mechanism, J. Photochem. Photobiol. C 10 (2009) 33–56.

[27] M. Zaier, L. Vidal, S. Hajjar-Garreau, L. Balan, Generating highly reflective and conductive metal layers through a light assisted synthesis and assembling of silver nanoparticles in a polymer matrix, Scientific Reports 7 (2017) 12410 DOI :10.103841598-017-121617-8

[28] L. Balan, J.-P. Malval, D.-J. Lougnot, In situ photochemically assisted synthesis of silver nanoparticles in polymer matrixes, Silver nanoparticles, David Pozo Perez Eds (2010) 79-91.

[29] J.-L. Philippart, C. Sinturel, J.-L. Gardette, Influence of light intensity on the photooxidation of polypropylene, Polym.Degrad. Stab. 58 (1997) 261-268.

[30] J.-L. Philippart, C. Sinturel, R. Arnaud, J.-L. Gardette, Influence of the exposure parameters on the mechanism of photooxidation of polypropylene, Polym.Degrad. Stab. 64 (1999) 213-225.

[31] J.-F. Larché, P.-O. Bussière, P. Wong-Wah-Chung, J.-L. Gardette, Chemical structure evolution of acrylic-melamine thermoset upon photo-ageing, Eur. Polym. J. 48 (2012) 172–182.

[32]T. Kumazawa, X.-P. Lee, K. Sato, O. Suzuki, Solid-phase microextraction and liquid chromatography/mass spectrometry in drug analysis, Anal. Chim. Acta 492 (2003) 49–67.

[33] M. Baba, J-L. Gardette, J. Lacoste, Crosslinking on ageing of elastomers: I. Photoageing of EPDM monitored by gel, swelling and DSC measurements, Polym. Degrad. Stab.63 (1999) 121-126.

[34] M. Baba, J-M. Nedelec, J. Lacoste, J-L. Gardette, M. Morel, Crosslinking of elastomers resulting from ageing: use of thermoporosimetry to characterise the polymeric network with n-heptane as condensate, Polym. Degrad. Stab. 80 (2003) 305-313.

[35] P-O. Bussière, B. Mailhot, A. Rivaton, M.-F. Barthe, J.-L. Gardette, M. Baba, Photocrosslinking of poly(N-vinylcarbazole): Implementing a complementary set of techniques to characterize the three-dimensional network formation, Polym. Degrad. Stab. 93 (2008)1376-1382.

[36] M.I.M Habib, Application des méthodes de l'analyse thermique à l'étude du vieillissement des polymers, PhD thesis Université Blaise Pascal Clermont-Ferrand, France (2013).

[37] S. Morlat, J.-L. Gardette, Phototransformation of water soluble polymers. I: photo- and thermooxidation of poly(ethylene oxide) in solid state, Polymer 42 (2001) 6071-6079.

[38] F. Hassouna, Etude des mécanismes de phototransformation de polymères hydrosolubles en milieu aqueux, PhD thesis Université Blaise Pascal Clermont-Ferrand, France (2006).

[39] C. Wilhelm, J.-L. Gardette, Infrared identification of carboxylic acids formed in polymer photooxidation, J. Appl. Polym. Sci. 51 (1994) 1411-1420.

[40] F. Kahabbaz, A.-C. Albertsson, S. Karlsson, Trapping of volatile low molecular weight photoproducts in inert and enhances degradable LDPE, Polym. Degrad. Stab. 61 (1998) 329-342.

[41] J.-H. Bortoluzzy, E.A. Pinheiro, E. Carasek, V. Soldi, Solid phase microextraction to concentrate volatile products from thermal degradation of polymers, Polym. Degrad. Stab. 89 (2005) 33-37.

[42] A. Lattuati-Derieux, S. Thao-Heu, B. Lavédrine, Assessment of the degradation of polyurethane foams after artificial and natural ageing by using pyrolysis-gas chromatography/mass spectrometry and headspace-solid phase microextraction-gas chromatography/mass spectrometry, J. Chromatogr. A 1218 (2011) 4498-4508.

[43] M.N. Mortensen, Stabilization of poly(ethylene glycol) in archeological wood, Ph.D. thesis Technical University of Denmark, Denmark (2009).

[44] S. Carroccio, P. Rizzarelli, C. Puglisi, G. Montaudo, MALDI investigation of photooxidation in aliphatic polyesters: poly(butylene succinate), Macromolecules 37 (2004) 6576-6586.

[45] J. Bei, W. He, X. Hu, S. Wang, Photodegradation behavior and mechanism of block copoly(caprolactone-ethylene glycol), Polym. Degrad. Stab. 67 (2000) 375-380.

[46] E.T. Tenório-Neto, M.R. Guilherme, M.E.G. Winkler, L. Cardozo-Filho, S.C. Beneti, A.F. Rubira, M.H. Kunita, Synthesis and characterization of silver nanoparticle nanocomposite thin films with thermally induced surface morphology changes, Materials Letters 159 (2015) 118-121.